

Complex Langevin: Etiology and Diagnostics of its Main Problem

Gert Aarts^{a†} Frank A. James^{a§} Erhard Seiler^{b||}
and Ion-Olimpiu Stamatescu^{c**}

^a*Department of Physics, Swansea University
Swansea, United Kingdom*

^b*Max-Planck-Institut für Physik (Werner-Heisenberg-Institut)
München, Germany*

^c*Institut für Theoretische Physik, Universität Heidelberg and FEST
Heidelberg, Germany*

Abstract

The complex Langevin method is a leading candidate for solving the so-called sign problem occurring in various physical situations. Its most vexing problem is that in some cases it produces ‘convergence to the wrong limit’. In the first part of the paper we go through the formal justification of the method, identify points at which it may fail and identify a necessary and sufficient criterion for correctness. This criterion would, however, require checking infinitely many identities, and therefore is somewhat academic. We propose instead a truncation to the check of a few identities; this still gives a necessary criterion, but a priori it is not clear whether it remains sufficient. In the second part we carry out a detailed study of two toy models: first we identify the reasons why in some cases the method fails, second we test the efficiency of the truncated criterion and find that it works perfectly at least in the toy models studied.

Keywords: finite density; complex Langevin

[†]email: g.aarts@swan.ac.uk

[§]email: pyfj@swan.ac.uk

^{||}email: ehs@mppmu.mpg.de

^{**}email: I.O.Stamatescu@thphys.uni-heidelberg.de

1 Introduction

The sign problems arising in simulations of various systems, in particular in QCD with finite chemical potential [1], are in principle solved by using the complex Langevin equation (CLE). This method, after being proposed in the early 1980s by Klauder [2] and Parisi [3], enjoyed a certain limited popularity (see for instance [4,5]) and has in more recent years been revived with some success [6–14]. Unfortunately already in the beginning problems were encountered. The first problem, instability of the simulations (runaways) can be dealt with by introducing an adaptive step size, as shown in [11]. More vexing is the second problem: convergence to a wrong limit [15–18]. It is this problem which we wish to address in this paper.

A formal argument for correctness of the CLE was presented in a previous paper [19]. It proceeded by comparing two time evolutions: the first one of a complex measure not allowing a probabilistic interpretation – the origin of the sign problem –, the other one of a positive measure on a complexified space, allowing a probabilistic interpretation and hence suitable for simulation. The main point was that, ignoring certain subtleties, these two time evolutions led to identical evolutions for the expectation values of holomorphic observables. This implied of course also that the long-time limits (assuming their existence) agreed, corresponding to the desired equilibrium expectation values.

In [19] we already identified some difficulties with those formal arguments. Some of them were of a slightly academic nature, namely the mathematically sticky problem of the existence of those evolutions and their convergence properties. Taking a pragmatic attitude, these problems are answered by performing simulations; in a large set of examples the answer is positive. The remaining problem is much more insidious: it may (and sometimes it does) happen that the results of a simulation are well converged and look perfectly fine, but turn out to be wrong when compared with known results. Of course in most interesting cases the results are not known and one would like to have a test to decide if one should trust the outcome of a simulation or not.

To deal with the disease of ‘convergence to the wrong limit’ it helps to have a deeper understanding of its causes – the etiology – before developing ways to diagnose it. The possible causes of the failure of the formal arguments are: insufficient falloff of the probability distribution in the imaginary directions and too strong growth of the (time-evolved) observables in the imaginary directions. They can invalidate the integrations by parts that are necessary to show agreement of the two time evolutions mentioned above. Section 2 revisits the formal argument and deduces a crucial identity (depending on the observable chosen) that has to be fulfilled if the two time evolutions are to agree.

Section 3 considers the long-time limits of the two time evolutions. Our set of

identities (one for each observable) leads in the long time limit to a set of simpler ones which turn out to be closely related to the Schwinger-Dyson equations. We show that in principle the complete set of these identities, together with a certain bound, is necessary and sufficient to establish correctness, provided some mild technical conditions are fulfilled. For practical purposes, however, the infinite set of identities has to be truncated to a finite (actually small) set; a proof of their sufficiency is thus no longer possible.

We then study these issues in detail in two toy models. The first one is a one-link version of lattice U(1) gauge theory, already studied in [9, 19]; the second one, which was first studied by Guralnik and Pehlevan [20], is a polynomial model with purely imaginary action, which is a toy version of the real time Feynman path integral. In this investigation we use noise both in the real and the imaginary directions, even though in principle real noise would be sufficient. The reason for this is twofold: it allows to study how and why the formal arguments can fail, and it gives us the possibility to approach the problem also in the dual way by solving the Fokker-Planck equation.

In Section IV we study the identity necessary for the agreement of the two time evolutions for the U(1) one-link model. In order to be able to do this with sufficient precision, we introduce a device that at first seems rather ad hoc: we introduce a periodic cutoff for the imaginary part of the field. But we can take advantage of the fact that a positive measure on the complexification of the original field space, required only to produce the right expectations for *holomorphic* observables, is not unique, so it is conceivable that a measure with cutoff gives correct results. With a cutoff we can compute the time evolution of the probability measure with high precision using the Fokker-Planck equation (FPE). The time evolution of the observables (averaged over the noise), is also needed; the way we define it here it does not depend on the cutoff. Of course the cutoff invalidates the formal argument, and as expected, we find that the two evolutions in general do not agree. But surprisingly it turns out that the cutoff can be tuned to a value that restores agreement.

But how can the formal argument fail when there is no cutoff? This is explained by looking at the growth of the (noise averaged) observables in imaginary direction, evolved for a finite amount of time. It turns out that these averages grow like an exponential of an exponential, a growth that cannot be compensated by the decay of the probability measure; so the formal argument becomes inapplicable.

In Section V we investigate for both toy models the falloff of the equilibrium distribution in imaginary direction; again it is found that in the presence of complex noise the falloff is insufficient for the derivation of the SDE identities. This corroborates the indications presented in [19]. On the other hand, for only real noise the distributions show much stronger falloff (actually they are concentrated

on a line in the $U(1)$ one-link model), which is sufficient for the derivation of the SDE identities.

Finally in Section VI we use a truncated form of our SDE criterion as a test of correctness of the equilibrium measures in both our toy models; it turns out that the test is surprisingly strong. To put it in terms of medical statistics: the test has perfect *specificity* (100%), i.e. when the simulation is correct, it is always fulfilled; this is a general mathematical fact. But the pleasant surprise is its very strong *sensitivity*, meaning that in the cases studied, when it is fulfilled, the results, as far as checked, are correct.

Here again we introduce a periodic cutoff for the imaginary part of the field variable. As in the finite time situation this can in general not be expected to work, because it destroys the formal argument for correctness, but again it turns out that in the two toy models studied here, the cutoff can be tuned to produce correct results. Requesting fulfillment of a few of the identities mentioned above is then used as a test for correctness: surprisingly we find not only that this test can be fulfilled by tuning the cutoff, but that in this case we obtain the correct expectation values. The same situation arises for real noise: the simulations pass the test and produce the right values. However, in lattice models the situation is not so simple and just suppressing imaginary noise is not always sufficient. This has already been found in the XY model [14]; in a separate paper [21] that model will be analyzed further from the point of view developed in this article.

Finally in Sec. 7 we draw some conclusions and present an outlook on work in progress.

2 The formal arguments revisited

We briefly go through the arguments presented in [19], concentrating on models in which the fields take values in flat manifolds $\mathcal{M}_r = \mathbb{R}^n$ or $\mathcal{M}_r = T^n$, where T^n is the n dimensional torus $(S^1)^n$ with coordinates (x_1, \dots, x_n) .

The complex measure $\exp(-S)dx$, with S a holomorphic function on a real manifold \mathcal{M} , is replaced by a positive measure $Pdxdy$ on the complexification \mathcal{M}_c of \mathcal{M} , which is the equilibrium measure of the complex Langevin process on \mathcal{M}_c ; the hope is that expectation values of *entire holomorphic observables* \mathcal{O} agree with those obtained using the complex measure $\exp(-S)dx$.

The complex Langevin equation (CLE) on \mathcal{M}_c is

$$\begin{aligned} dx &= K_x dt + \sqrt{N_R} dw_R, \\ dy &= K_y dt + \sqrt{N_I} dw_I, \end{aligned} \tag{1}$$

where dw_R and dw_I are independent Wiener processes, $N_I \geq 0$ and $N_R = N_I + 1$.

In the case $N_I > 0$ we speak of complex noise. The drift is given by

$$\begin{aligned} K_x &= -\operatorname{Re}\nabla_x S(x + iy), \\ K_y &= -\operatorname{Im}\nabla_x S(x + iy). \end{aligned} \quad (2)$$

By Itô calculus, if f is a twice differentiable function on \mathcal{M}_c and

$$z(t) = x(t) + iy(t) \quad (3)$$

is a solution of the complex Langevin equation (1), we have

$$\frac{d}{dt} \langle f(x(t), y(t)) \rangle = \langle Lf(x(t), y(t)) \rangle, \quad (4)$$

where L is the Langevin operator

$$L = [N_R \nabla_x + K_x] \nabla_x + [N_I \nabla_y + K_y] \nabla_y, \quad (5)$$

and $\langle f \rangle$ denotes the noise average of f corresponding to the stochastic process described by Eq. (1). In the standard way Eq. (1) leads to its dual Fokker-Planck equation (FPE) for the evolution of the probability density $P(x, y; t)$,

$$\frac{\partial}{\partial t} P(x, y; t) = L^T P(x, y; t), \quad (6)$$

with

$$L^T = \nabla_x [N_R \nabla_x - K_x] + \nabla_y [N_I \nabla_y - K_y]. \quad (7)$$

L^T is the formal adjoint (transpose) of L with respect to the bilinear (not hermitian) pairing

$$\langle P, f \rangle = \int f(x, y) P(x, y) dx dy, \quad (8)$$

i.e.,

$$\langle P, Lf \rangle = \langle L^T P, f \rangle. \quad (9)$$

To understand the relations between the real and the complex measures one has to consider the evolution of a complex density $\rho(x)$ on \mathcal{M} under the following complex FPE

$$\frac{\partial}{\partial t} \rho(x; t) = L_0^T \rho(x; t), \quad (10)$$

where now the complex Fokker-Planck operator L_0^T is

$$L_0^T = \nabla_x [\nabla_x + (\nabla_x S(x))]. \quad (11)$$

We will also use a slight generalization: For any $y_0 \in \mathcal{M}$ we consider the complex Fokker-Planck operator $L_{y_0}^T$ given by

$$L_{y_0}^T = \nabla_x [\nabla_x + (\nabla_x S(x + iy_0))]. \quad (12)$$

$L_{y_0}^T$ is the formal adjoint of

$$L_{y_0} = [\nabla_x - (\nabla_x S(x + iy_0))] \nabla_x. \quad (13)$$

The complex density

$$\rho(x; \infty) \propto \exp[-S(x)] \quad (14)$$

is a stationary solution of Eq. (10), which is expected to be unique. Numerical studies (where feasible) of Eq. (10) confirm this; in fact the convergence to the limit Eq. (14) seems to be exponentially fast.

We have to make a few technical remarks about the space of observables we choose: all observables have to be entire holomorphic functions; we will furthermore require that their restrictions to the real submanifold \mathcal{M}_r span a large enough space \mathcal{D} :

(1) if $\mathcal{M}_r = T^n$, \mathcal{D} should be a dense subset of $\mathcal{C}(\mathcal{M}_r)$, the set of all continuous functions on \mathcal{M} equipped with the norm $\|\mathcal{O}\| \equiv \sup_x |\mathcal{O}(x)|$; a good choice is the space of finite linear combinations of exponentials.

(2) if $\mathcal{M}_r = \mathbb{R}^n$ and the action S has a real part that grows at least like $|x|$ as $|x| \rightarrow \infty$, the functions in $\mathcal{O} \in \mathcal{D}$ should be bounded polynomially and dense in the Banach space defined by the norm $\|\mathcal{O}\| \equiv \sup_x \exp(-|x|) |\mathcal{O}(x)|$; a natural choice for \mathcal{D} is the space of polynomials.

(3) if $\mathcal{M}_r = \mathbb{R}^n$ and the action is purely imaginary, one has to find a submanifold $\mathcal{M}'_r \subset \mathcal{M}_c$ which is a suitable deformation of \mathcal{M}_r into the complex domain, such that the integral of $\exp(-S)$ converges and \mathcal{M}'_r can still be parameterized by $x \in \mathbb{R}^n$. The conditions on the observables, expressed in this parameterization are then as in (2). In a slight abuse of language, we still refer to \mathcal{M}'_r as the ‘real submanifold’. Again polynomials are a natural choice for the space of observables.

We set

$$\langle \mathcal{O} \rangle_{P(t)} \equiv \frac{\int O(x + iy) P(x, y; t) dx dy}{\int P(x, y; t) dx dy} \quad (15)$$

and

$$\langle \mathcal{O} \rangle_{\rho(t)} \equiv \frac{\int O(x) \rho(x; t) dx}{\int \rho(x; t) dx}. \quad (16)$$

What one would like to show is that

$$\langle \mathcal{O} \rangle_{P(t)} = \langle \mathcal{O} \rangle_{\rho(t)}, \quad (17)$$

if the initial conditions agree,

$$\langle \mathcal{O} \rangle_{P(0)} = \langle \mathcal{O} \rangle_{\rho(0)}, \quad (18)$$

which is assured provided

$$P(x, y; 0) = \rho(x; 0)\delta(y - y_0). \quad (19)$$

One expects that in the limit $t \rightarrow \infty$ the dependence on the initial condition disappears by ergodicity.¹

To establish a connection between the ‘expectation values’ with respect to ρ and P for a suitable class of observables, one moves the time evolution from the densities to the observables and makes use of the Cauchy-Riemann (CR) equations. Formally, i.e. without worrying about boundary terms and existence questions, this works as follows: first we use the fact that we want to apply the complex operators L_{y_0} only to functions that have analytic continuations to all of \mathcal{M}_c . On those analytic continuations we may act with the Langevin operator

$$\tilde{L} \equiv [\nabla_z - (\nabla_z S(z))] \nabla_z, \quad (20)$$

whose action on holomorphic functions agrees with that of L , since on such functions $\nabla_y = i\nabla_x$ and $\Delta_x = -\Delta_y$ so that the difference $L - \tilde{L}$ vanishes.

We now use \tilde{L} to evolve the observables according to the equation

$$\partial_t \mathcal{O}(z; t) = \tilde{L} \mathcal{O}(z; t) \quad (t \geq 0) \quad (21)$$

with the initial condition $\mathcal{O}(z; 0) = \mathcal{O}(z)$, which is formally solved by

$$\mathcal{O}(z; t) = \exp[t\tilde{L}] \mathcal{O}(z). \quad (22)$$

In Eqs. (21, 22), because of the CR equations, the tilde may be dropped, and we will do so now. So we also have

$$\mathcal{O}(z; t) = \exp[tL] \mathcal{O}(z). \quad (23)$$

In [19] it was shown that $\mathcal{O}(z; t)$ is holomorphic if $\mathcal{O}(z; 0)$ is. The evolution can therefore also be obtained equivalently by solving

$$\partial_t \mathcal{O}(x + iy_0; t) = L_{y_0} \mathcal{O}(x + iy_0; t) \quad (t \geq 0) \quad (24)$$

and subsequent analytic continuation.

The crucial object to consider is, for $0 \leq \tau \leq t$,

$$F(t, \tau) \equiv \int P(x, y; t - \tau) \mathcal{O}(x + iy; \tau) dx dy, \quad (25)$$

which interpolates between the ρ and the P expectations:

$$F(t, 0) = \langle \mathcal{O} \rangle_{P(t)}, \quad F(t, t) = \langle \mathcal{O} \rangle_{\rho(t)}. \quad (26)$$

¹In [13] dependence on initial conditions was found to be due to peculiar features of the classical flow pattern, leading to degenerate equilibrium distributions.

The first equality is obvious, while the second one can be seen as follows, using Eqs. (19, 23),

$$\begin{aligned}
F(t, t) &= \int P(x, y; 0) (e^{tL} \mathcal{O}) (x + iy; 0) dx dy \\
&= \int \rho(x; 0) (e^{tL_0} \mathcal{O}) (x; 0) dx \\
&= \int \mathcal{O}(x; 0) (e^{tL_0^T} \rho) (x; 0) dx \\
&= \langle \mathcal{O} \rangle_{\rho(t)},
\end{aligned} \tag{27}$$

where it is only necessary to assume that integration by parts in x does not produce any boundary terms.

The desired result Eq. (17) would follow if $F(t, \tau)$ were independent of τ . To check this, we take the τ derivative:

$$\begin{aligned}
\frac{\partial}{\partial \tau} F(t, \tau) &= - \int (L^T P(x, y; t - \tau)) \mathcal{O}(x + iy; \tau) dx dy \\
&\quad + \int P(x, y; t - \tau) L \mathcal{O}(x + iy; \tau) dx dy.
\end{aligned} \tag{28}$$

Integration by parts, if applicable without boundary term at infinity, then shows that the two terms cancel, hence $\frac{\partial}{\partial \tau} F(t, \tau) = 0$ and thus proves Eq. (17), irrespective of N_I .

So here we have found a place where the formal argument may fail: if the decay of the product

$$P(x, y; t - \tau) \mathcal{O}(x + iy; \tau) \tag{29}$$

and its derivatives is insufficient for integration by parts without boundary terms.

If (28) vanishes and furthermore

$$\lim_{t \rightarrow \infty} \langle \mathcal{O} \rangle_{\rho(t)} = \langle \mathcal{O} \rangle_{\rho(\infty)}, \tag{30}$$

with $\rho(\infty)$ given by Eq. (14), one can conclude that the expectation values of the Langevin process relax to the desired values. Eq. (30) requires that the spectrum of $L_{y_0}^T$ lies in a half plane $\text{Re } z \leq 0$ and 0 is a nondegenerate eigenvalue. (Actually, convergence of $P(x, y; t)$ is more than what is really needed, because the measure will only be tested against holomorphic observables.)

The numerical evidence in practically all cases points to the existence of a unique stationary probability density $P(x, y; \infty)$. More detailed information about this will be given below.

In [19] three questions were raised. The first one concerned the exponentiation of the operators L, \tilde{L} and their transposes, or in other words whether they are

generators of semigroups on some suitable space of functions. Even though we have not found a general mathematical answer to this question, numerics indicate that it is affirmative in all cases considered; for L_{y_0} in our first toy model a proof will be given in Sec. 4. Likewise it is not known whether the spectra of L, L_{y_0} are contained in the left half plane and if 0 is a nondegenerate eigenvalue, but the numerics again strongly indicate an affirmative answer.

So the main remaining question concerns the integrations by parts without boundary terms, which underlie the shifting of the time evolution from the measure to the observables and back; actually what is really needed is the ensuing τ independence of $F(t, \tau)$, defined in Eq. (25).

A crucial role for the correctness of CLE simulations is therefore played by the vanishing of (28). Whether this holds or not will be studied in detail for one of our toy models in Section 6.

3 A criterion for correctness

As explained in the previous section, $F(t, \tau)$ has to be independent of τ for all times t , i. e.

$$\frac{\partial}{\partial \tau} F(t, \tau) = 0. \quad (31)$$

Below in Section IV it will be seen that for the U(1) one-link model the τ derivative is largest at $\tau = 0$. This motivates to try the superficially weaker condition

$$\lim_{t \rightarrow \infty} \left. \frac{d}{d\tau} F(t, \tau) \right|_{\tau=0} = 0. \quad (32)$$

We will see later that this condition is in fact still sufficient for correctness, modulo some technical conditions, if it holds for a sufficiently large set of observables.

If we now look again at Eq. (28), we realize that for the equilibrium measure (always assuming it exists) $L^T P(x, y; \infty) = 0$ and hence the first term on the right hand side vanishes. The criterion (32) thus turns into

$$E_{\mathcal{O}} \equiv \int P(x, y; \infty) \tilde{L}\mathcal{O}(x + iy; 0) dx dy = \langle \tilde{L}\mathcal{O} \rangle = 0, \quad (33)$$

where we used the fact that on \mathcal{O} L and \tilde{L} can be used interchangeably. This would of course also follow from the equilibrium condition $L^T P(x, y; \infty) = 0$ on \mathcal{M}_c , if the decay of P at large y is sufficient to allow integration by parts on \mathcal{M}_c without boundary term. Eq. (33) is a fairly simple condition that is rather easy to check for a given observable. But it has to be satisfied for ‘all’ observables i.e. for a basis (in a suitable sense) of our chosen space \mathcal{D} , so it represents really an infinite tower of identities.

It may be worth noting that the collection of identities (33), applied to all observables, is closely related to the Schwinger-Dyson equations (SDE). We show this for the simple case of a scalar theory on a lattice with fields denoted by ϕ_i : the SDEs are well-known to arise from the relation

$$\left\langle \frac{\partial f}{\partial \phi_i} \right\rangle = \left\langle f \frac{\partial S}{\partial \phi_i} \right\rangle \quad (34)$$

for ‘any’ function f of the fields (in most applications the observables are chosen to be exponentials $\exp(\sum_i \phi_i j_i)$). Our Langevin criterion $\langle \tilde{L}\mathcal{O} \rangle$ on the other hand reads

$$\sum_i \left\langle \frac{\partial^2 \mathcal{O}}{\partial \phi_i^2} \right\rangle = \sum_i \left\langle \frac{\partial \mathcal{O}}{\partial \phi_i} \frac{\partial S}{\partial \phi_i} \right\rangle. \quad (35)$$

It is quite obvious that Eq. (34) implies Eq. (35): we only have to set in Eq. (34) $f = \partial_i \mathcal{O}$. The converse is also easy: we only have to find a set of observables \mathcal{O}_j satisfying

$$\sum_i \frac{\partial^2 \mathcal{O}_j}{\partial \phi_i^2} = \partial_j f; \quad (36)$$

this involves just inversion of the (functional) Laplace operator, which is always possible here, because the only zero modes are constants.

We proceed to show that in principle the identities for a sufficiently large (countably infinite) set of observables are also sufficient to assure correctness, provided a certain bound is satisfied. Let us now assume that we have, by whatever method, obtained a measure Q on \mathcal{M}_c that allows integration of all $\mathcal{O} \in \mathcal{D}$ and furthermore satisfies a bound

$$|\langle Q, \mathcal{O} \rangle| \leq C \|\mathcal{O}\|, \quad (37)$$

where C is some constant and the norm is the one discussed in Section II (recall that this norm only involved the values of \mathcal{O} on \mathcal{M}_r). We claim that modulo certain technical conditions the fulfillment of Eq. (33) for a basis of \mathcal{D} ,

$$\langle Q, \tilde{L}\mathcal{O} \rangle = \int Q(x, y) \tilde{L}\mathcal{O}(x + iy) dx dy = 0, \quad (38)$$

implies that the Q expectations are correct, i.e.

$$\langle Q, \mathcal{O} \rangle = \int Q(x, y) \mathcal{O}(x + iy) dx dy = \frac{1}{Z} \int_{\mathcal{M}_r} \mathcal{O}(x) e^{-S(x)} dx. \quad (39)$$

The argument uses the fact that the values of \mathcal{O} on \mathcal{M}_r already determine the values on \mathcal{M}_c . So $\langle Q, \mathcal{O} \rangle$ can be viewed as a linear functional on the space \mathcal{D} considered as functions on \mathcal{M}_r , which is assumed to be dense in $\mathcal{C}(\mathcal{M}_r)$. Because of the bound Eq. (37) this functional has a unique extension to a linear functional

on all of $\mathcal{C}(\mathcal{M}_r)$. By a standard theorem of analysis – the Riesz-Markov theorem (see for instance [22]) – this linear functional is therefore given by a complex measure $\sigma_Q dx$ on \mathcal{M} , i.e. we can write

$$\langle Q, \mathcal{O} \rangle = \int_{\mathcal{M}_r} \mathcal{O}(x) \sigma_Q(x) dx, \quad (40)$$

where σ_Q is allowed to contain δ functions. Since \mathcal{O} was any observable, we may replace it by $\tilde{L}\mathcal{O}$; we then have

$$\langle Q, \tilde{L}\mathcal{O} \rangle = \int_{\mathcal{M}_r} (\tilde{L}\mathcal{O})(x) \sigma_Q(x) dx = 0, \quad (41)$$

which is equivalent to

$$\int_{\mathcal{M}_r} \mathcal{O}(x) (L_0^T \sigma_Q)(x) dx = 0, \quad (42)$$

using only integration by parts on \mathcal{M}_r , which in general unproblematic. Since this holds for all \mathcal{O} in the dense set \mathcal{D} , we conclude

$$L_0^T \sigma_Q = 0. \quad (43)$$

To deduce from this that $\sigma_Q = \exp(-S)/Z$ we only need that 0 is a nondegenerate eigenvalue of L^T , an assumption we had to make anyway in Section II. In concrete models this needs checking, of course.

If, on the other hand, we find $E_{\mathcal{O}} \neq 0$ for some observable \mathcal{O} , this means that our simulation is not correct. Since by formal integration by parts on \mathcal{M}_c the equilibrium condition $L^T P(x, y; \infty) = 0$ would imply $E_{\mathcal{O}} = 0$, we can see only one possible reason for $E_{\mathcal{O}} \neq 0$, namely insufficient falloff of the equilibrium measure in imaginary direction.

This whole discussion is a bit superficial, as far as the functional analysis is concerned, but it is not worth going into more detail here, since it is quite academic anyway. In practice it will be difficult to check the bound Eq. (37) (see however Section VI) and impossible to check the criterion for a full basis of observables; we are reduced to checking it for a few. So the sensitivity of the resulting test needs to be checked experimentally.

It is well known that the SDE's have spurious, unphysical solutions (see for instance [23], [7] or [24]). This should be obvious from the fact that they are equivalent to a (functional) differential equation which requires at least some kind of boundary conditions for definiteness and also from the fact that they are *recursive* relation that can always be fulfilled by fixing the low moments/modes in an arbitrary way. So it has to be checked whether requiring the criterion Eq. (33) in fact selects the correct expectation values. The bound Eq. (37) will in general be sufficient for this. In Section 6 we will see how this works in the U(1) one-link model.

4 Detailed study of $F(t, \tau)$ for the U(1) one-link model

4.1 Numerical study

The U(1) one-link model was introduced in [9] and studied further in [19]. At lowest order in the hopping expansion it is defined by the action

$$S = -\beta \cos z - \kappa \cos(z - i\mu) = -a \cos(z - ic), \quad (44)$$

with

$$a = \sqrt{(\beta + \kappa e^\mu)(\beta + \kappa e^{-\mu})}, \quad (45)$$

$$c = \frac{1}{2} \ln \frac{\beta + \kappa e^\mu}{\beta + \kappa e^{-\mu}}, \quad (46)$$

leading to the drift

$$K_x = -\text{Re } S' = -a \sin x \cosh(y - c), \quad (47)$$

$$K_y = -\text{Im } S' = -a \cos x \sinh(y - c). \quad (48)$$

It is easy to see by shifting an integration contour that no essential generality is lost if we set $c = 0$. So in the sequel we will make this choice. We will also set $a = 1$.

A natural choice of a basis for the space of observables are the exponentials e^{ikz} . Here we study in detail the question whether the quantity $F(\tau, t)$, see Eq. (25), is indeed independent of τ , as required for correctness. We use both CLE and FPE for this analysis; since the former yields ambiguous results for $k > 1$ if $N_I > 0$, whereas the latter requires $N_I > 0$ for stability (see below), we are forced to introduce a field cutoff in this analysis. We are aware of the fact that such a cutoff destroys the formal argument for correctness, but using the nonuniqueness of the positive measure on \mathcal{M}_c there is still a chance to get correct results with such a measure; we will check whether it is possible by tuning the cutoff.

We introduce the cutoff in the simplest possible way by imposing periodic boundary conditions in field space. In our U(1) one-link model we have periodic b.c. in the x direction by definition, so we only have to cut off the imaginary part; we denote the value of the cutoff by Y , such that $-Y \leq y \leq Y$. Periodizing the observable of course violates the Cauchy-Riemann (CR) equations at the ‘seam’, while the drift becomes discontinuous across the ‘seam’ making the interpretation of the FPE also difficult. But quite independent of those issues, if Eq. (31) holds the equality Eq. (17) follows and thus the correctness of the CLE method is assured.

In any case we will see that our rather naive cutoff procedure seems to be justified to some extent by its success.

We present the results of a numerical evolution of the function $F(t, \tau)$, choosing the simplest observable $\mathcal{O} = \exp(iz)$ and the parameter $N_I = 0.1$. To do this, both the evolution of the probability density P (see Eq. (6)) and the evolution of the observable (see Eqs. (21),(24)) are needed.

$P(x, y; t - \tau)$ is obtained by using the time dependent FPE in the Fourier representation; a simple Euler discretization in time with time step 10^{-5} turns out to be sufficient. This was discussed already in some detail in [19].

$\mathcal{O}(x + iy; \tau)$ is obtained as described in the previous section (Eqs. (21),(24)) by using the evolution of \mathcal{O} under \tilde{L} or equivalently under L_{y_0} . This evolution does not depend on either N_I or the cutoff Y , since neither L nor L_{y_0} depend on those two parameters.

$F(t, \tau)$ is then obtained by summing up the products of $\mathcal{O}(x + iy; t)$ and $P(x, y; t - \tau)$. The results are presented in Figs. 1, 2, 3, 4.

In these plots we show $F(t, \tau)$ as a function of τ , for a number of t values, ranging from $t = 1$ to $t = 7$. For every t value, τ runs from 0 to t . In all cases $N_I = 0.1$, while the cutoff Y varies from $Y = 3.162$ in Fig. 1 to $Y = 0.158$ in Fig. 3.

The following features can be seen from the figures:

- (1) In general $F(t, \tau)$ is *not* independent of τ ,
- (2) the dependence is always strongest at $\tau = 0$,
- (3) the sign of the τ derivative changes somewhere between $Y = 0.474$ and $Y = 1.582$; there seems to be a ‘best choice’ of cutoff at which the derivative vanishes.

This picture is corroborated by Fig. 5, which shows directly the τ derivatives obtained as finite difference approximations. In this figure we also show different values of N_I and it is clearly visible that for very small values of N_I the derivative also effectively vanishes. Note that $N_I = 0$, which should be preferred for a CLE simulation, cannot be used for the FPE computations, because it would lead to instabilities (see Section VIB below).

4.2 Mathematical analysis of the failure

In this subsection we analyze in more detail the behavior of the time evolved observables in order to understand why in general $F(t, \tau)$ is not independent of τ .

We describe the evolution of the observables in some more detail: the Langevin

operator \tilde{L} is

$$\tilde{L} = \frac{d^2}{dz^2} - a \sin(z - ic) \frac{d}{dz}. \quad (49)$$

For the observables e^{ikz} we find

$$\tilde{L}e^{ikz} = -k^2 e^{ikz} - \frac{a}{2} k (e^c e^{i(k+1)z} - e^{-c} e^{i(k-1)z}). \quad (50)$$

Choosing now $c = 0$ and $a = \beta$, we consider an observable

$$\mathcal{O}(z) = \sum_k a_k e^{ikz} \quad (51)$$

and its time evolution $\mathcal{O}(z; t) \equiv \sum_k a_k(t) e^{ikz}$ defined by Eq. (21). This evolution can be expressed in terms of the coefficients a_k as follows:

$$\partial_t a_k(t) = -k^2 a_k(t) + \frac{\beta}{2} [-(k-1)a_{k-1}(t) + (k+1)a_{k+1}(t)] \quad (52)$$

and may be viewed as evolution under \tilde{L} , L or, if we fix $y = 0$, as evolution under L_0 . The evolution operator L_0 in Fourier space is thus represented by a tridiagonal matrix with elements

$$(\hat{L}_0)_{kk'} = -k^2 \delta_{kk'} + \frac{\beta}{2} [-(k-1)\delta_{k-1,k'} + (k+1)\delta_{k+1,k'}]. \quad (53)$$

We now establish the following facts:

- (1) The Langevin operators L_{y_0} generate exponentially bounded semigroups on the Hilbert space $L^2(dx)$ for any y_0 . In particular there are no poles.
- (2) If the Fourier transform of \mathcal{O} contains only positive modes, this will also be true for $\exp(tL_{y_0})\mathcal{O}$. But typically then all positive modes will be populated.
- (3)

$$\lim_{t \rightarrow \infty} e^{tL_{y_0}} \mathcal{O} = \frac{1}{Z_{y_0}} \int dx \mathcal{O}(x + iy_0) e^{-S(x + iy_0)} \quad (54)$$

and the convergence is exponentially fast.

- (4) For holomorphic observables \mathcal{O}

$$\exp(tL)\mathcal{O} = \exp(tL_{y_0})\mathcal{O}. \quad (55)$$

Since the right hand side is independent of $N_I = N_R - 1$, so is the left hand side. This argument does not involve any integration by parts.

- (5) $\mathcal{O}(x + iy; t)$ grows for $t > 0$ more strongly than any exponential as $y \rightarrow \infty$, invalidating integration by parts except for $N_I = 0$.

The proof of (1) follows from a theorem to be found in [25] (Theorem 11.4.5). The point is that the drift (first order in derivatives) term of L_{y_0} is a so-called Phillips perturbation of the Laplacian:

$$L_{y_0} = A + B, \quad (56)$$

with

$$A = \frac{d^2}{dx^2}, \quad B = \beta \sin(x + iy_0) \frac{d}{dx}. \quad (57)$$

B can be applied to any vector of the form $\exp(tA)\psi$, $t > 0$ and we have

$$\int_0^1 dt \|B \exp(tA)\| < \infty. \quad (58)$$

These two properties allow to set up a perturbation expansion for $\exp[t(A + B)]$ and show its convergence. Explicitly

$$e^{t(A+B)} = e^{tA} + \sum_{n=1}^{\infty} \int_{0 \leq t_1 \leq \dots \leq t_n \leq t} e^{t_1 A} B e^{(t_2 - t_1)A} B \dots B e^{(t - t_n)A}. \quad (59)$$

Convergence in norm is not hard to see: by Fourier transformation one sees that

$$\left\| \frac{d}{dx} e^{tA} \right\| = \sup_k |ke^{-tk^2}| \leq \frac{1}{\sqrt{2te}}, \quad (60)$$

hence

$$\|Be^{tA}\| \leq \text{const } \beta e^{|y_0|} \frac{1}{\sqrt{t}}. \quad (61)$$

From this it is obvious that the bound (58) holds; since the integration volume in Eq. (58) is $t^n/n!$, the series converges in norm;

(2) is obvious;

(3) means in particular that the evolution of \mathcal{O} converges to a constant. While it is obvious that all constants are eigenfunctions of L_{y_0} , we don't have sufficient analytic understanding of the spectra of the operators L_{y_0} to prove this convergence. Numerically, however, it is seen easily that the evolution converges to the correct constant and the convergence is exponentially fast;

(4) is an obvious consequence of analyticity;

(5) is seen by numerically analyzing the growth of the coefficients $a_k(t)$ for $t > 0$:

Using the initial condition $a_1 = 1$, $a_k = 0$ for $k \neq 0$ and $\beta = 1$ as before, $a_k(t)$ are the Fourier coefficients of $\exp(tL_0)\mathcal{O}_1$ with $\mathcal{O}_1(x) = \exp(ix)$. In Fig. ref{growth} we plot $-\ln(|a_k(t)|)/k$ for four different times ($t = 0.5, 1, 2, 3$) against $\ln(k)$. As remarked, only positive modes get populated; it turns out that the coefficients

$a_k(t)$ alternate in sign. From this we conclude that $|\mathcal{O}_1(z; t)|$ grows most for large negative y and is maximal for $x = \pm\pi$. Modes were cut off at $|k| = 50$, but the picture shows for all the times clearly an asymptotic linear increase with a slope close to 1, so we conclude

$$a_k(t) \sim K^k (-1)^k k^{-\gamma k}, \quad (62)$$

with γ possibly slightly less than 1 and some constant K . Further numerical studies show that the behavior of Eq. (62) is universal: it is independent of the initial condition and β . For comparison in this figure we also show (in black) the quantity $\ln(k!)/k + \ln(2)$, which seems to be approached asymptotically by the other curves.

Since Eq. (62) obviously implies

$$|a_k(t)| \geq K^k k^{-k}, \quad (63)$$

by a simple argument we can conclude that $\mathcal{O}(x+iy; t)$ grows superexponentially in y direction: we put $w = e^z$; then, using only positive modes for the initial conditions, $\mathcal{O}(z; t)$ is given by the power series

$$\mathcal{O}(z; t) = \sum_{k=0}^{\infty} a_k(t) w(z)^k. \quad (64)$$

Cauchy's estimate says that for any $R \geq 0$

$$|a_k(t)| \leq S(R) R^{-k}, \quad (65)$$

where

$$S(R) = \sup_{|w|=R} |\mathcal{O}(z(w); t)| = \sup_x |\mathcal{O}(x - i \ln R; t)|. \quad (66)$$

From this and our numerics we conclude that asymptotically

$$S(R) \geq (KR)^k k^{-k} \quad (67)$$

and this holds for any k . The optimal value is

$$k_0 = (KR)e^{-1}, \quad (68)$$

which leads to the bound

$$S(e^{-y}) = |\mathcal{O}(\pi + iy)| \geq \exp[\text{const} \exp(-y)]. \quad (69)$$

Note that this holds in particular for $y < 0$! Since for $N_I > 0$ and $t, \tau > 0$ one can at best expect a Gaussian decay of $P(x, y; t)$, Eq. (25) in this case involves an integral of a function that is not absolutely integrable and hence its value is ambiguous, depending on the order of integrations. Thus the formal argument for correctness of the CLE fails.

5 Falloff of equilibrium measures

In this section we study the $t \rightarrow \infty$ limit of $P(x, y; t)$, i.e. the equilibrium measure in order to check why and how our general criterion Eq. (33) can fail. As remarked in Section 3, the equilibrium condition

$$L^T P(x, y; \infty) = 0 \quad (70)$$

implies fulfillment of the criterion

$$E_{\mathcal{O}} \equiv \int P(x, y; \infty) \tilde{L} \mathcal{O}(x + iy; 0) dx dy = 0, \quad (71)$$

provided integration by parts on \mathcal{M}_c without boundary terms at imaginary infinity is justified. So the falloff of $P(x, y; \infty)$ is crucial for success or failure.

5.1 U(1) one-link model

For the U(1) one-link model studied in [9, 19] we are able to make rather precise statements about the falloff of the equilibrium measure in the y direction.

The system is symmetric under the reflections $x \mapsto -x$ and $y - c \mapsto -(y - c)$. To study the falloff of the equilibrium measure in y we again chose $c = 0$ and grouped the data obtained by the CLE simulation into bins $|y| \in [(n - 1/2)\epsilon, (n + 1/2)\epsilon]$ with $\epsilon = 0.1$. For clarity we chose rather large values of $N_I = 0.1, 0.5, 1.0$ and 9.0. The results are shown in Fig. 7 and show clearly a universal decay rate

$$P(x, y; \infty) \sim \exp(-2|y|). \quad (72)$$

This result improves considerably the statement made in [19] and also explains the difficulties with determining reliably expectation values of $\exp(ikz)$ for $|k| \geq 2$ (they are suffering from extremely large fluctuations).

In [19] we considered the Fourier modes

$$\hat{P}_k(y; t) = \int dx e^{ikx} P(x, y; t); \quad (73)$$

formally the expectation values of the exponentials are given by

$$\langle e^{ikz} \rangle = \int dy \hat{P}_k(y; t) e^{-ky}, \quad (74)$$

using the fact that

$$\int dy \hat{P}_k(y; t) = \int dx dy P(x, y; t) = 1. \quad (75)$$

We simplify the notation for $\widehat{P}_k(y; \infty)$ to $\widehat{P}_k(y)$. By binning in y as above we also produced estimates of the modes $\widehat{P}_k(y)$ for $k = 1, 2$ and $N_I = 1$, shown in Fig. 8. \widehat{P}_2 seems already to be quite noisy, but at least the first few kinks visible in the figure for \widehat{P}_2 correspond to true sign changes. But what is more important is the clearly visible fact that \widehat{P}_1 and \widehat{P}_2 decay at least like $\exp(-3|y|)$. This can be confirmed using the stationary Fokker-Planck equation (FPE) obeyed by $P(x, y; \infty)$. In terms of the Fourier modes the FPE reads (see Eq. (65) of [19]):

$$(N_R k^2 - N_I \partial_y^2) \widehat{P}_k(y) + \frac{\beta}{2} \cosh(y) \left[(k-1) \widehat{P}_{k-1}(y) - (k+1) \widehat{P}_{k+1}(y) \right] - \frac{\beta}{2} \sinh(y) \partial_y \left[\widehat{P}_{k-1}(y) + \widehat{P}_{k+1}(y) \right] = 0. \quad (76)$$

Since we are interested in the large $|y|$ asymptotics, we may replace $\cosh(y)$ and $\sinh(y)$ by $\pm 1/2 \exp(|y|)$. Integrating Eq. (76) for $k = 0$ from 0 to y and using evenness in y we obtain

$$N_I \widehat{P}'_0(y) + \frac{\beta}{2} e^{|y|} \widehat{P}_1(y) = 0. \quad (77)$$

So if \widehat{P}_0 decays like $\exp(-2|y|)$, \widehat{P}_1 will decay like $\exp(-3|y|)$. Continuing inductively and assuming exponential decay, one obtains easily

$$\widehat{P}_k(y) \sim c_k e^{-(|k|+2)|y|}. \quad (78)$$

Unfortunately Eq. (76) also implies that $c_{k+1} \sim kc_k$, which means that one cannot sum up the asymptotic behavior of the \widehat{P}_k to obtain the asymptotics of $P(x, y; \infty)$.

More important is what we learn about the expectation values of $\exp(ikz)$, which should be given by

$$\langle e^{ikz} \rangle = \int P(x, y; \infty) e^{ikx - ky} dx dy. \quad (79)$$

The integral on the right hand side does not converge absolutely for $|k| \geq 2$, hence its value is ambiguous. A well defined result may be obtained by first integrating over x , but it is not clear if this corresponds to the long time average of the complex Langevin process. But it seems that the large fluctuations observed in the CLE data reflect the fact that the integral is ill defined.

One can also try to compute expectation values using the binning employed above. This corresponds to first integrating over x , then over y . The results, however, agree with those obtained directly by the CLE simulation (up to some loss of precision due to the finite width of the bins) and not to the exact values. This is of course no surprise, as the binning is based on the CLE simulation.

The conclusion is that the CLE process with complex noise and without a field cutoff will in general not produce unambiguous results for the expectation values of exponentials $\exp(ikz)$ with higher $|k|$.

5.2 The model of Guralnik and Pehlevan

To see if this phenomenon of slow decay of the equilibrium distribution is not just a specialty of our $U(1)$ one-link model, we also analyzed the equilibrium measure for the simplest polynomial model (called GP model in the sequel), studied already by Guralnik and Pehlevan [20] and discussed briefly in [19].

The model is defined by the action

$$S = -i\beta \left(z + \frac{1}{3}z^3 \right); \quad (80)$$

since this action is purely imaginary, we have to deform the real axis to a path (submanifold) \mathcal{M}_r as described in Section II such that $\exp(-S)$ is absolutely integrable over \mathcal{M}_r . A possible choice (cf. [20]) is the path $z = x + i\epsilon\sqrt{1+x^2}$ for some small positive ϵ .

Since the action produces a stable fixed point at $x = 0, y = 1$, we produced histograms representing $P(x, y; \infty)$ by binning $r = \sqrt{x^2 + (y-1)^2}$ in intervals of length 0.1. They are shown in Fig. 9. Since in this case we expect a power falloff, we use a log-log scale. The indications are again that the rate of falloff is the same for different values of $N_I > 0$, namely roughly like $r^{-1.5}$, whereas for $N_I = 0$ we find a stronger falloff (we cannot decide at this point whether it is still power-like or stronger).

Accepting this observation one concludes that for $N_I > 0$ again the higher moments $\langle z^k \rangle$ of the equilibrium distribution are ill-defined, a fact that is reflected by large fluctuations of these quantities in the CLE simulations [19].

6 Testing the criterion

We now proceed to test the truncated version of our criterion on the two toy models introduced; our primary interest is to see whether checking it only for a few low moments (modes) is sufficient to identify incorrect results.

6.1 $U(1)$ one-link model

For this model we considered the two cases

$$\beta = 1, \quad \kappa = 0 \quad (81)$$

and

$$\beta = 1, \quad \kappa = 0.25, \quad \mu = 0.5 \quad (82)$$

(which is equivalent to $\beta \approx 1.27$, $\kappa = 0$). In both cases we chose $N_I = 0.1$ which was found in [19] to lead to manifestly incorrect results for the CLE simulation without cutoff. Using the FPE as well as the CLE simulations, we measured the expectation values $\langle \exp(iz) \rangle$ and $\langle \exp(2iz) \rangle$ as well as the corresponding quantities $\langle \tilde{L} \exp(iz) \rangle$ and $\langle \tilde{L} \exp(2iz) \rangle$. Again we introduced a periodic cutoff Y in imaginary direction which stabilizes the FPE solution as well as the CLE expectation values.

In Figs. 10 and 11 we show $\langle \mathcal{O}_k \rangle$ divided by its exact value minus 1 and E_k , both for $k = 1, 2, 3$. The results indicate the remarkable fact that at a particular value of the cutoff not only all the indicators

$$E_k \equiv \langle \tilde{L} \exp(ikz) \rangle \quad (83)$$

vanish but also

$$c_k \equiv \langle \mathcal{O}_k \rangle = \langle \exp(ikz) \rangle \quad (84)$$

agree with their exact values (it should be noted that due to the symmetry of the system the observables $\exp(-iz)$ and $\exp(-2iz)$ do not contain any extra information). Note that E_2 has a second zero, but at that point $E_1 \neq 0$.

So in this case our simple test of the identity (33) for two observables is apparently sufficient to identify the correct simulation: it has sufficient sensitivity to reject wrong solutions. To make sure that at the properly tuned cutoff value the measure P is indeed correct, one would in principle have to check all exponentials, again a practical impossibility.

In our U(1) one-link model the SDE hierarchy amounts just to the well known recursion relation for the Bessel functions $I_k(\beta)$ and it is determined by fixing $\langle 1 \rangle = 1$ and $\langle \exp(iz) \rangle = c_1$. In a CLE simulation c_1 will depend on the value of the cutoff. If

$$c_1 \neq \frac{I_1(\beta)}{I_0(\beta)}, \quad (85)$$

the SDE recursion rapidly runs away to infinity and it is manifest that the bound Eq. (37) cannot hold. So this bound seems to be crucial for picking out the right solution of the SDE. On the other hand the cutoff models in general obey the bound, but unless the cutoff is tuned correctly, they will miss the right value of c_1 and fail to obey the SDE recursion.

6.2 Guralnik-Pehlevan model

We next apply our test to our other toy model, the cubic model of Guralnik and Pehlevan. Since this model has noncompact real and imaginary parts, we introduce *two* periodic cutoffs: X for the real and Y for the imaginary part.

In this model $\tilde{L} = \partial_z^2 + i\beta(1+z^2)\partial_z$, and the first few relations read

$$\begin{aligned} E_1 &\equiv \langle \tilde{L}z \rangle = i\beta \langle 1+z^2 \rangle \\ E_2 &\equiv \langle \tilde{L}z^2 \rangle = 2\langle 1+i\beta z(1+z^2) \rangle \\ E_3 &\equiv \langle \tilde{L}z^3 \rangle = 3\langle 2z+i\beta z^2(1+z^2) \rangle, \end{aligned} \quad (86)$$

leading to SD relations between the expectation values of z^k .

It is easy to see that the exact results, which can be expressed in terms of Airy functions (see [20]) and for $\beta = 1$ are $\langle z \rangle \approx 1.1763i$, $\langle z^2 \rangle = -1$, $\langle z^3 \rangle \approx -0.1763i$, indeed satisfy these relations.

We measured the moments $c_k \equiv \langle z^k \rangle$ for $k = 1, 2, 3, 4$; this allows also to obtain $E_2 = \langle \tilde{L}z^2 \rangle$ and $E_3 = \langle \tilde{L}z^3 \rangle$; note that $E_1 = \langle \tilde{L}z \rangle = i + i\langle z^2 \rangle = 0$ is already tested by comparing $\langle z^2 \rangle$ to its exact values -1 . In Fig. 12 we present the results obtained for $N_I = 1$ and a fixed cutoff $X = 3.17$ in x direction, both by using the FPE and the CLE simulation. For this value of N_I it was observed already in [19] that CLE without cutoff does *not* reproduce the correct values. The figure, on the other hand, shows that there is a value of the y cutoff (near $Y = 0.8$) for which the two criteria $E_2 = E_3 = 0$ are fulfilled and also the right values for the moments c_1, c_2, c_3, c_4 are obtained.

With purely real noise ($N_I = 0$) the situation is quite different. For this case the FPE simulation is unstable: Fig. 13 shows the time evolution of the FPE for $N_I = 0$; the evolution settles onto metastable values very close to the exact ones, but then takes off and diverges. For comparison we also show the FPE time evolutions for two rather small nonzero values: $N_I = 0.01$ and $N_I = 0.1$ (all three figures are using the cutoffs $X = Y \approx 3.95$). As seen in Figs. 13, 14, the small imaginary noise is sufficient to stabilize the evolution, at least for the times considered. This seems to conform at least qualitatively to the discussion found in Numerical Recipes Ch. 19 [26]. Quantitatively from that discussion one would expect that much larger values N_I would be needed for stabilization; we are lucky that this does not seem to be the case here and in fact with this small nonzero N_I we obtain good convergence to the exact result, provided the cutoff is not extremely small.

The CLE simulation, on the other hand, works perfectly for $N_I = 0$. We have seen already in Section 3 that for $N_I = 0$ the equilibrium distribution is quite well concentrated and shows a very strong falloff. In agreement with this, we find that the data are quite insensitive to the cutoffs introduced; for $X = 3.95$ as before, even a cutoff of $Y = 0.8$ is sufficient to produce values close to the exact ones and consequently also fulfill the criteria $E_1 = E_2 = E_3 = 0$ with good precision. These facts can be clearly seen in Fig. 15; in this figure we display for comparison the CLE results for $N_I = 0$ and the FPE results for $N_I = 0.01$ (recall that $N_I = 0$ does not allow for a viable FPE solution).

Again we found that our simple test seems to have sufficient sensitivity to select the right simulation.

7 Conclusions and outlook

In this paper we have pinned down the reasons why the CLE simulations sometimes fail to produce correct expectation values and we have developed practical tests for correctness. In two toy models we checked the strength of the test, by deforming the process through introduction of complex noise ($N_I > 0$) as well as cutoffs. It turned out that our tests are successful in picking out the correct results.

In the context of this paper the introduction of a nonzero N_I plays a double role:

- (1) As a means to check the applicability of the formal proofs for correctness of the CLE.
- (2) As a parameter which can be used for tuning and stabilizing the simulation. As such it is needed in FPE computations, but for true lattice models, where there is little chance to use the FPE anyway, it is probably still best to stay with $N_I = 0$. The periodic field cutoff introduced in the toy models should be seen in a similar way.

One should not, however, expect that this simple device of tuning a cutoff will work in general to produce correct results. Other modifications might be necessary, but the most promising choice is still to work with the unmodified CLE process and purely real noise.

The main point is that our results demonstrate the ‘sensitivity’ of the truncated test criterion, in addition to the ‘specificity’ which holds on general grounds.

While we studied here only two very simple models, we believe the reasons for incorrect results identified here apply much more generally. They are:

- rapid growth of the Langevin evolved observables in imaginary direction,
- slow decay of the equilibrium distribution.

The study of the issues discussed in this paper will be continued; both the etiology and the diagnostics will be studied in the XY model [21] and in nonabelian models [27].

Acknowledgments

I.-O. S. thanks the MPI for Physics München and Swansea University for hospitality. G. A. and F. A. J. are supported by STFC.

References

- [1] P. de Forcrand, PoS **LAT2009** (2009) 010. [arXiv:1005.0539 [hep-lat]].
- [2] J. Klauder, Acta Phys. Austriaca Suppl. **XXXV** (1983) 251; J. Phys. A: Math. Gen. **16**, L317-319 (1983); Phys. Rev. A **29**, 2036-2047 (1984).
- [3] G. Parisi, Phys. Lett. B **131** (1983) 393.
- [4] F. Karsch and H. W. Wyld, Phys. Rev. Lett. **55** (1985) 2242.
- [5] P. H. Damgaard and H. Hüffel, Phys. Rept. **152** (1987) 227.
- [6] J. Berges and I.-O. Stamatescu, Phys. Rev. Lett. **95** (2005) 202003 [hep-lat/0508030].
- [7] J. Berges, S. Borsanyi, D. Sexty and I. O. Stamatescu, Phys. Rev. D **75** (2007) 045007 [hep-lat/0609058].
- [8] J. Berges and D. Sexty, Nucl. Phys. B **799** (2008) 306 [0708.0779 [hep-lat]].
- [9] G. Aarts and I.-O. Stamatescu, JHEP **0809** (2008) 018 [0807.1597 [hep-lat]].
- [10] G. Aarts, Phys. Rev. Lett. **102** (2009) 131601 [0810.2089 [hep-lat]].
- [11] G. Aarts, F. A. James, E. Seiler and I. O. Stamatescu, Phys. Lett. B **687** (2010) 154 [arXiv:0912.0617 [hep-lat]].
- [12] G. Aarts, JHEP **0905** (2009) 052 [0902.4686 [hep-lat]].
- [13] G. Aarts and K. Splittorff, JHEP **1008** (2010) 017 [arXiv:1006.0332 [hep-lat]].
- [14] G. Aarts and F. A. James, JHEP **1008** (2010) 020 [arXiv:1005.3468 [hep-lat]].
- [15] J. Ambjorn and S. K. Yang, Phys. Lett. B **165**, 140 (1985).
- [16] J. R. Klauder and W. P. Petersen, J. Stat. Phys. 39 (1985) 53.
- [17] H. Q. Lin and J. E. Hirsch, Phys. Rev. B **34** (1986) 1964.
- [18] J. Ambjorn, M. Flensburg and C. Peterson, Nucl. Phys. B **275**, 375 (1986).
- [19] G. Aarts, E. Seiler and I. O. Stamatescu, Phys. Rev. D **81** (2010) 054508 [arXiv:0912.3360 [hep-lat]].
- [20] G. Guralnik and C. Pehlevan, Nucl. Phys. B **822**, 349 (2009) [arXiv:0902.1503 [hep-lat]].

- [21] G. Aarts, F. James, E. Seiler and I. O. Stamatescu, in preparation.
- [22] M. Reed and B. Simon *Functional Analysis* vol. I, New York and London: Academic Press 1972.
- [23] E. Seiler, *Untersuchung eines selbstgekoppelten relativistischen Skalarfeldes mit Funktionalmethoden*, Doctoral thesis (Technische Universität München 1971), unpublished (in German).
- [24] C. Pehlevan and G. Guralnik, Nucl. Phys. B **811**, 519 (2009) [arXiv:0710.3756 [hep-th]].
- [25] E. B. Davies, Linear Operators and their Spectra, Cambridge University Press, Cambridge, UK 2007.
- [26] W. H. Press et al, “Numerical Recipes in Fortran 77 – The Art of Scientific Computing”, Second Edition, Ch. 19, Cambridge University Press, Cambridge 1992.
- [27] G. Aarts, F. James, E. Seiler, D. Sexty and I. O. Stamatescu, in preparation.

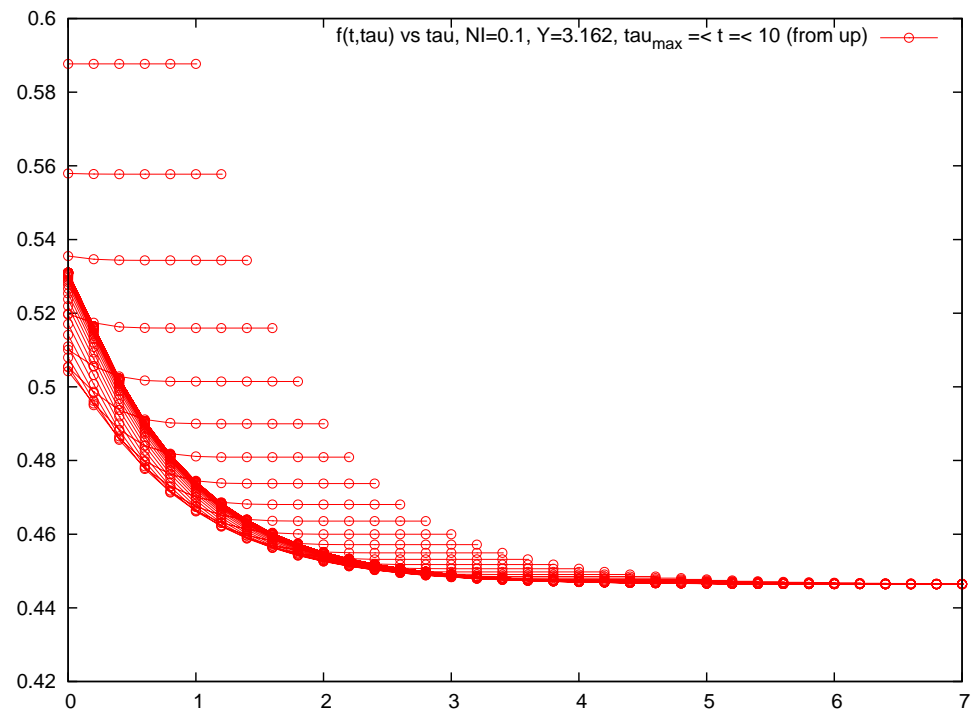


Figure 1: $F(t, \tau)$ vs. τ for several values of t , with $0 < \tau < t$, $N_I = 0.1$ and the cutoff $Y = 3.162$.

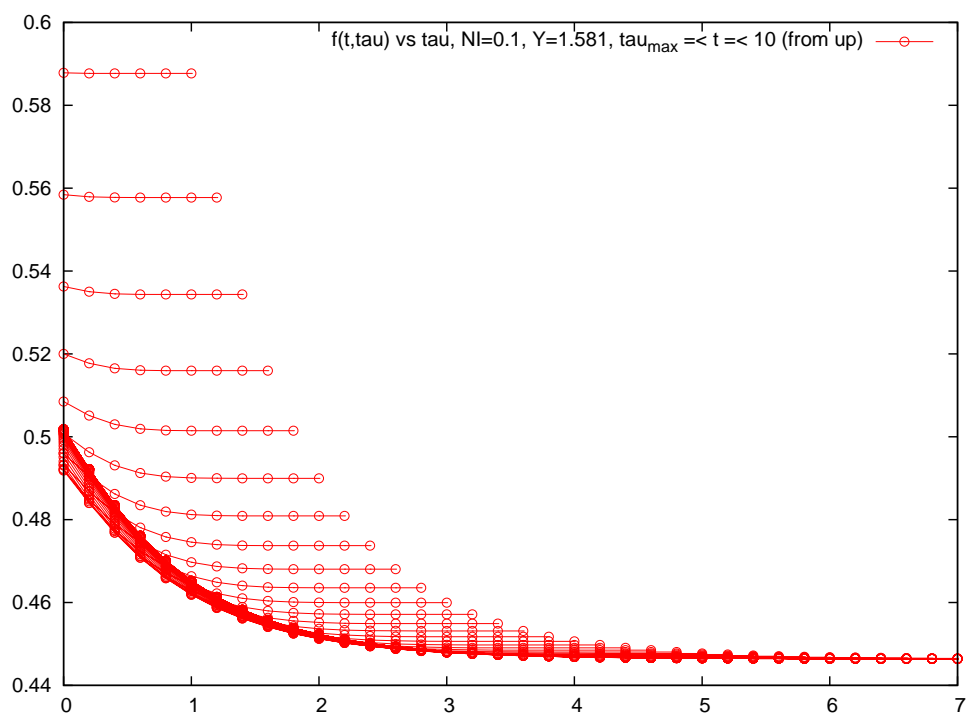


Figure 2: As in Fig. 1, with $Y = 1.582$.

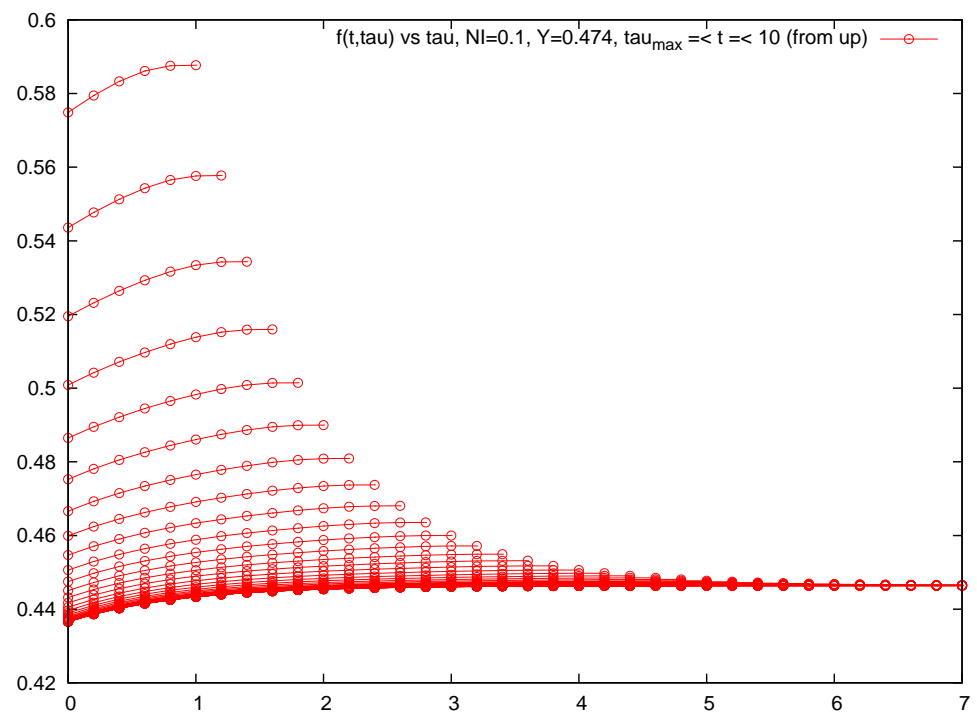


Figure 3: As in Fig. 1, with $Y = 0.474$

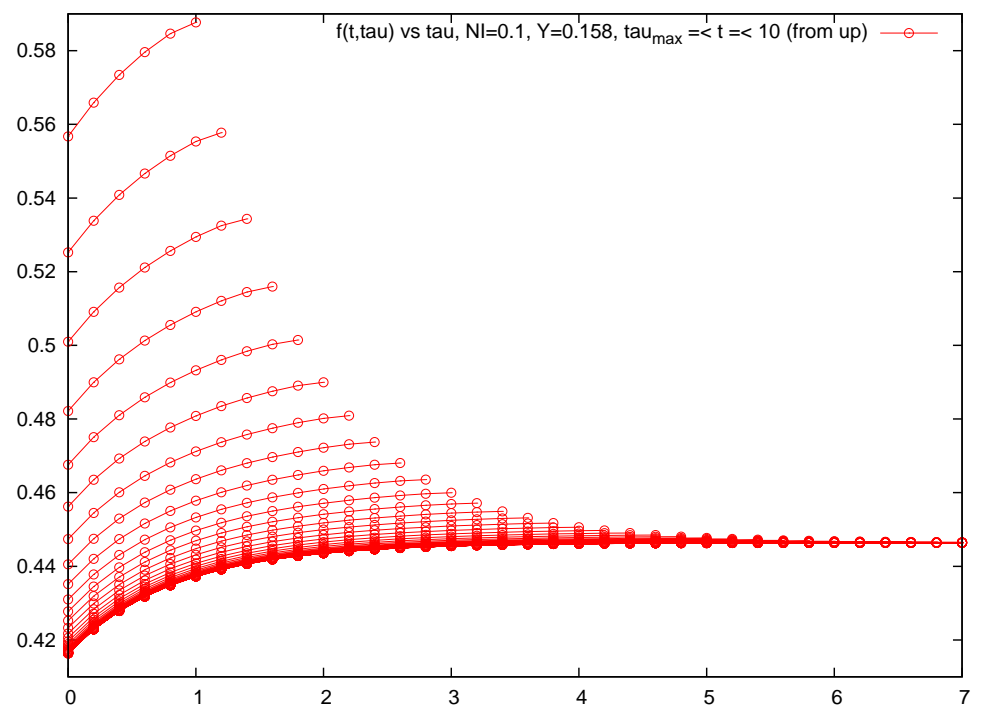


Figure 4: As in Fig. 1, with $Y = 0.158$.

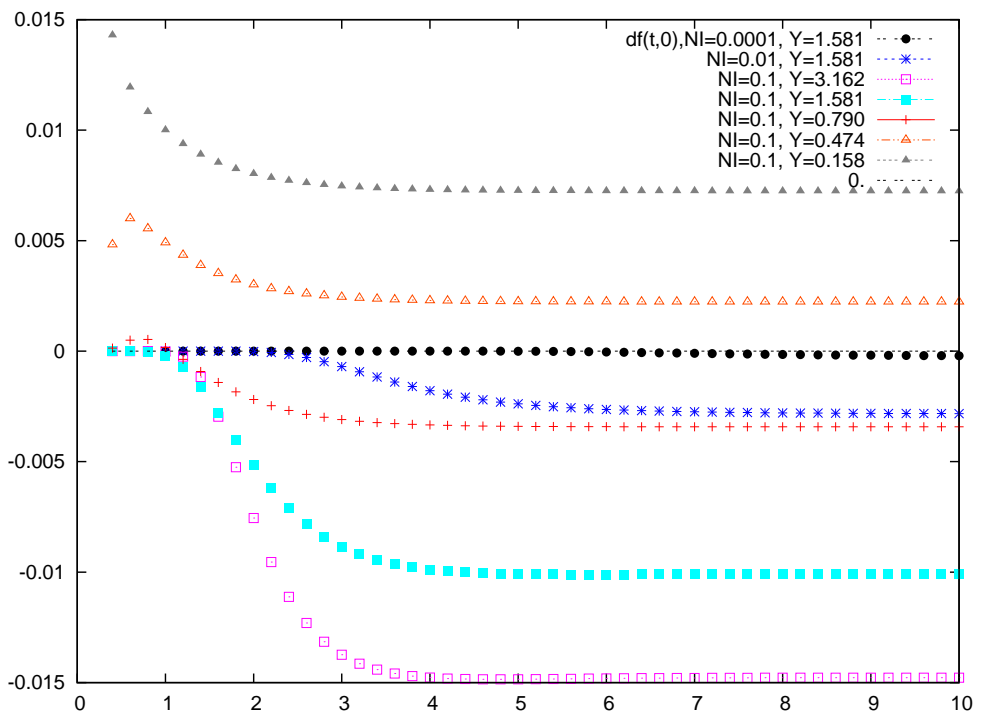


Figure 5: τ derivative of $F(t, \tau)$ as a function of τ at $t = 10$ for several values of the cutoff Y and complex noise parameter N_I .

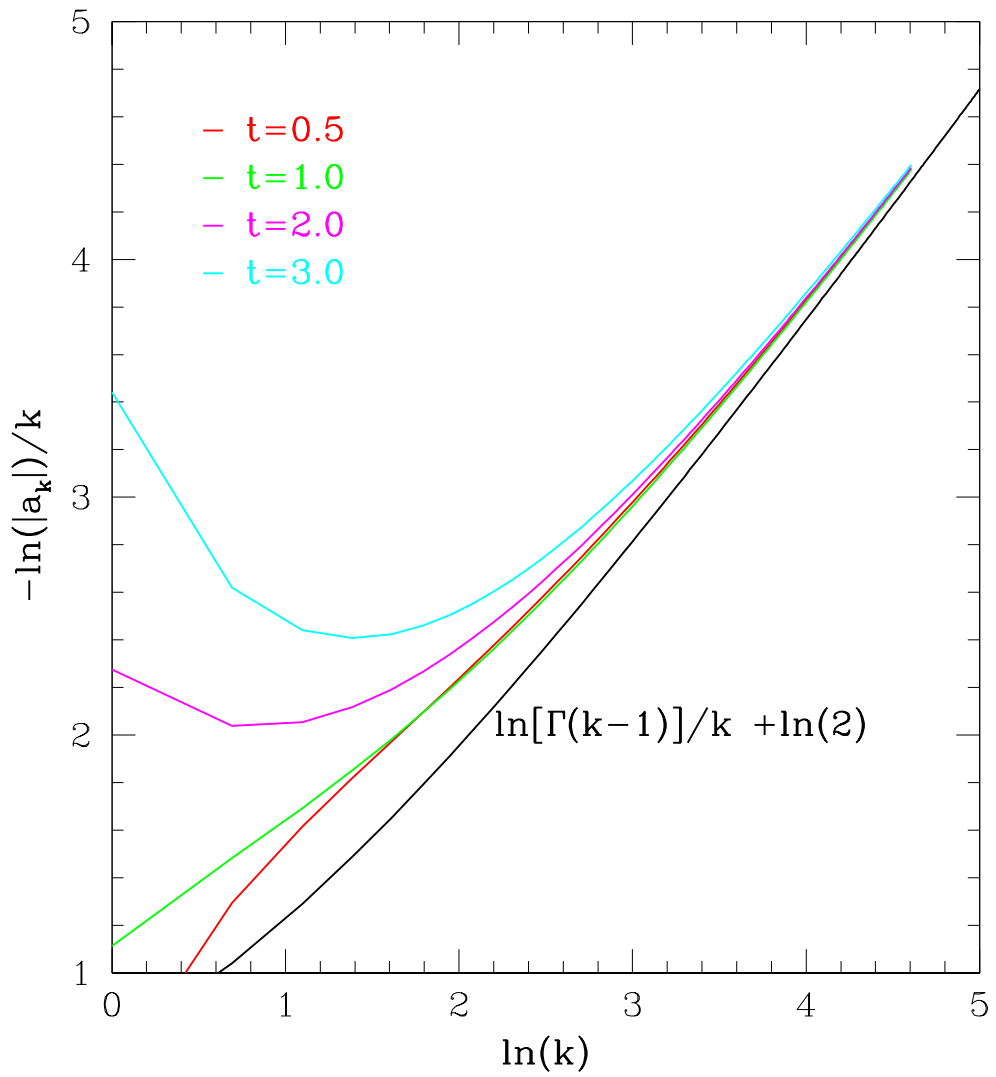


Figure 6: Asymptotics of the Fourier coefficients $a_k(t)$.

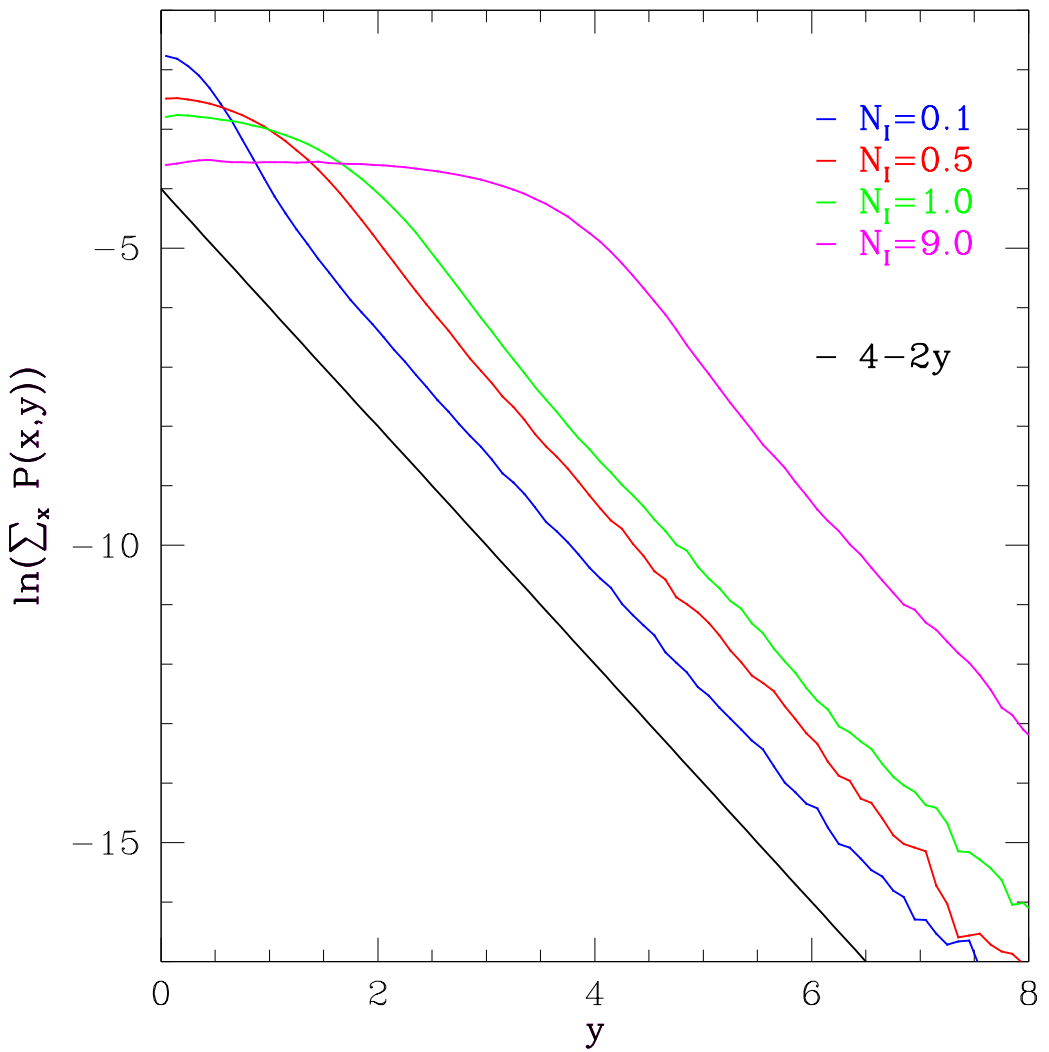


Figure 7: Logarithmic histograms of the equilibrium measures for the U(1) one-link model.

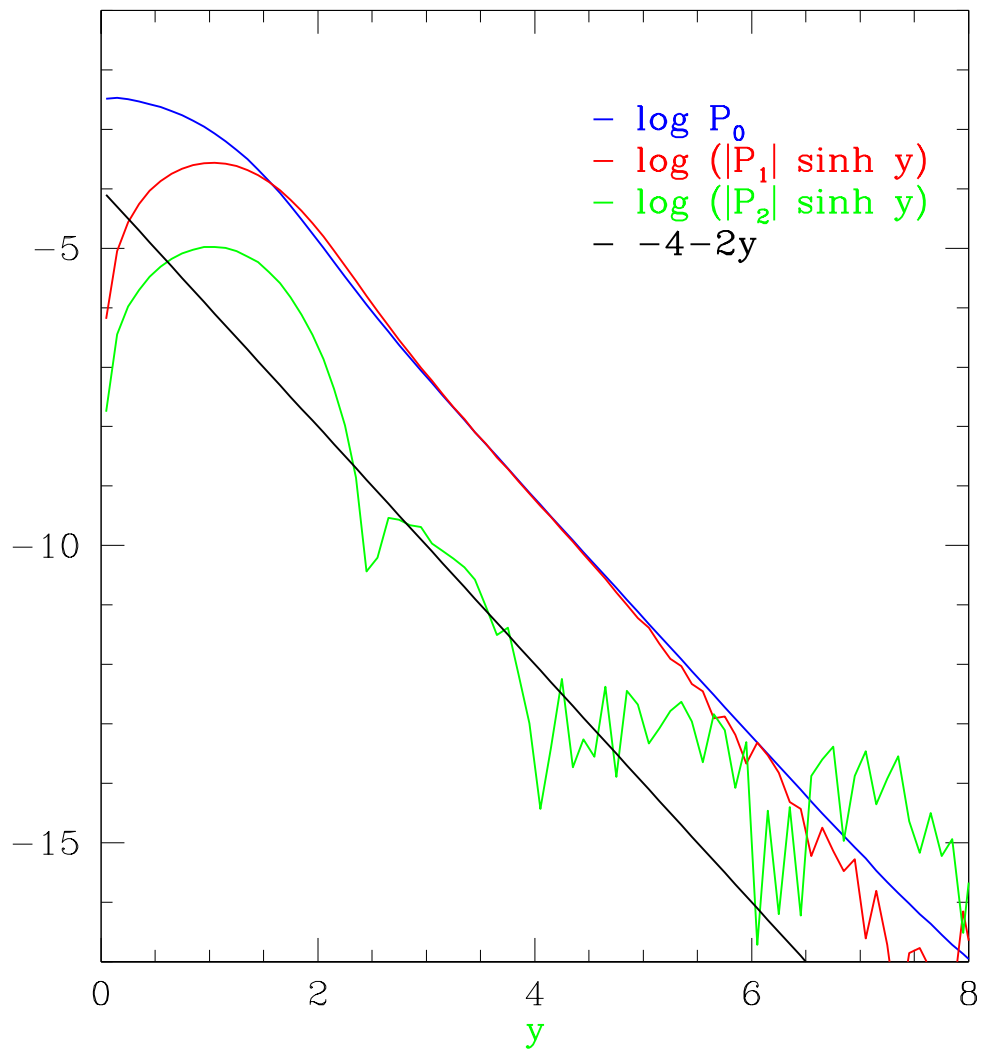


Figure 8: Logarithmic histograms of the low modes of the equilibrium measures for the U(1) one-link model.

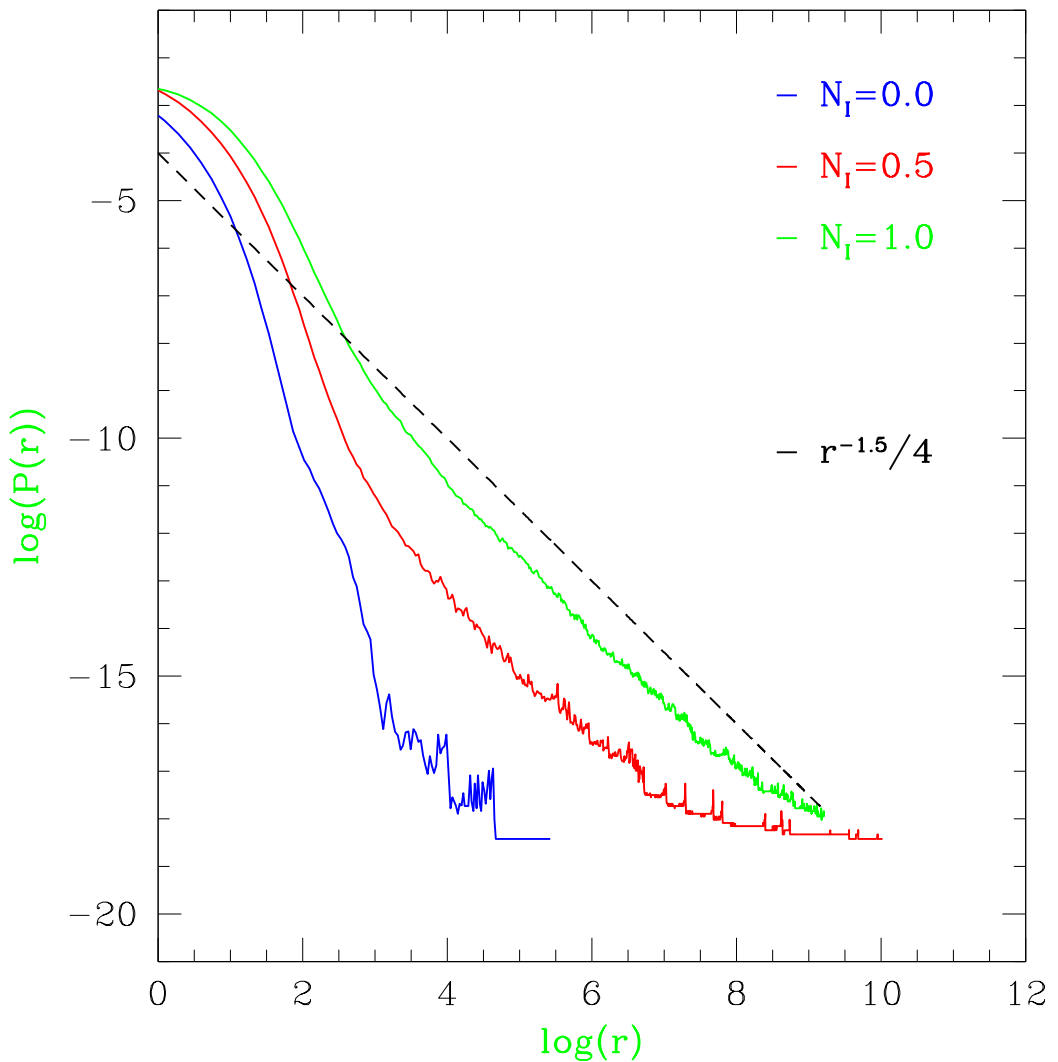


Figure 9: Histograms of the equilibrium measures for the GP model on a log-log scale.

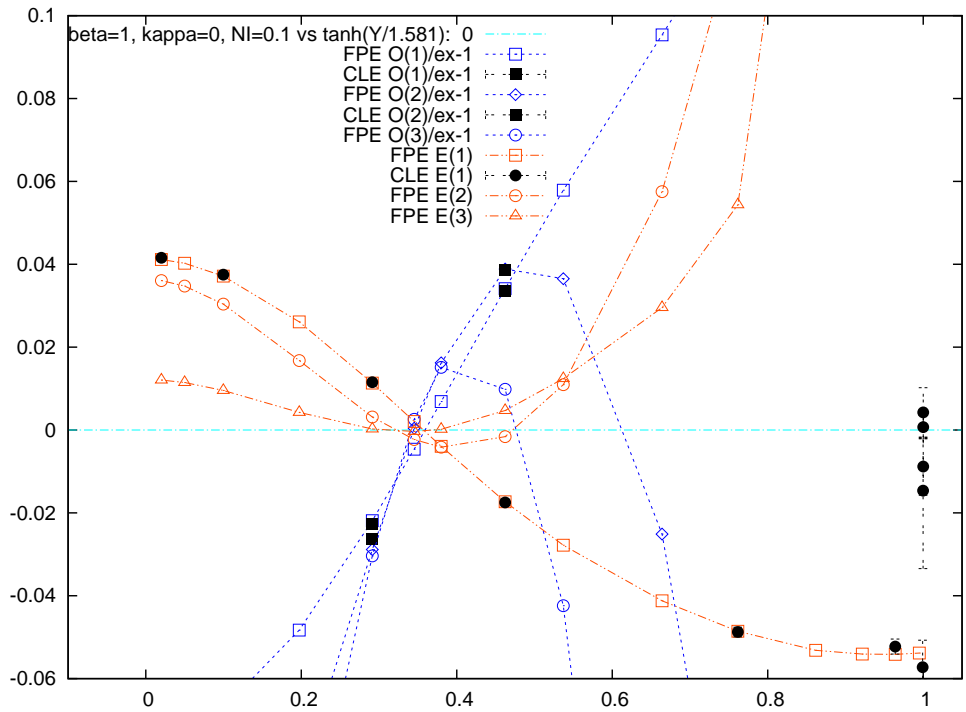


Figure 10: Cutoff (Y) dependence of various quantities in the $U(1)$ one-link model, for $\beta = 1$, $\kappa = 0$, $N_I = 0.1$. See main text for further details.

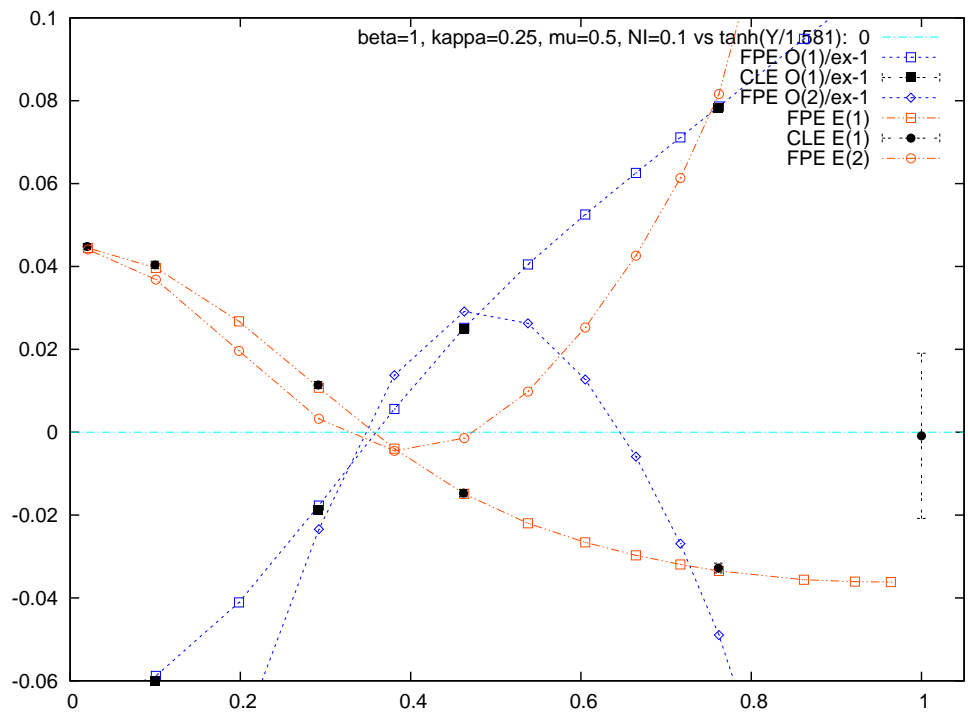


Figure 11: As in Fig. 10, for $\beta = 1$, $\kappa = 0.25$ and $\mu = 0.5$.

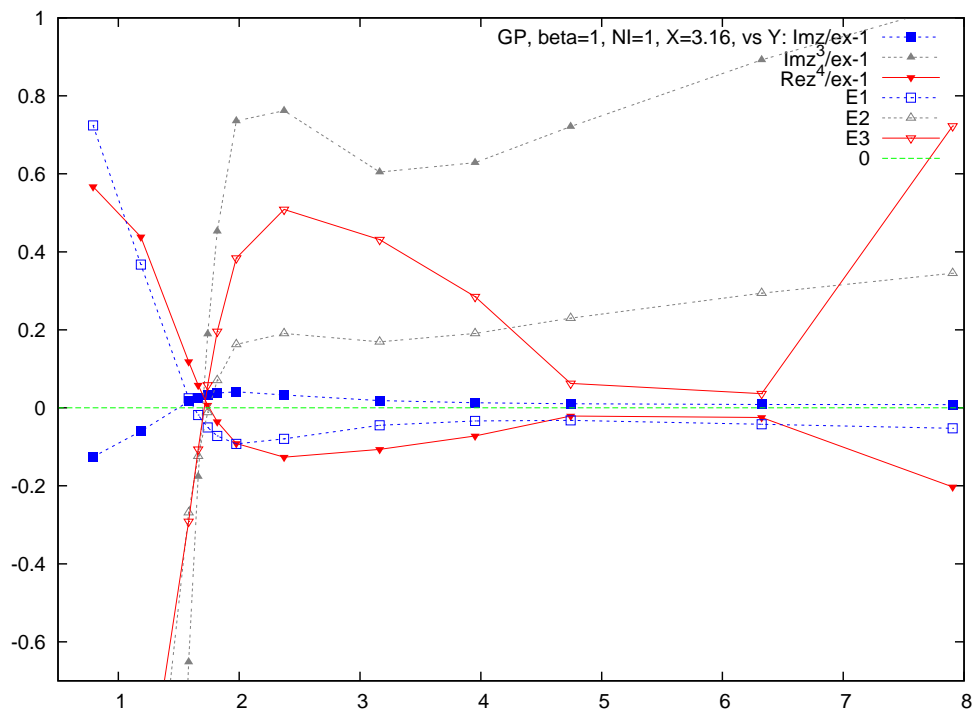


Figure 12: GP model: Cutoff dependence for $\beta = 1, N_I = 1$.

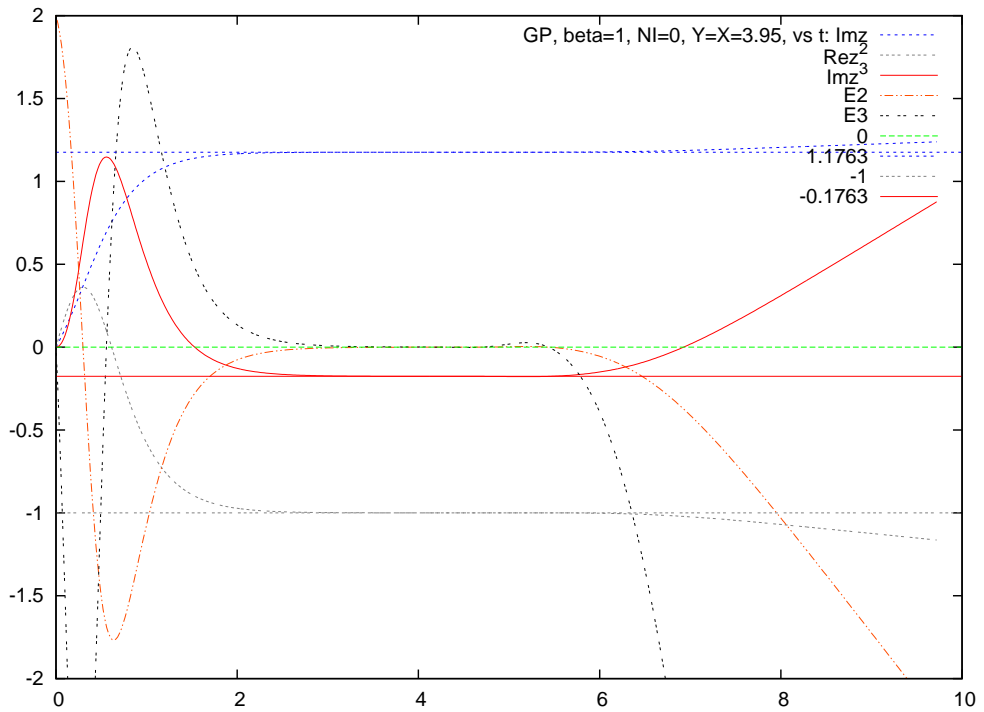


Figure 13: FPE evolution in the GP model: t dependence of various quantities for $N_I = 0$, $\beta = 1$ and cutoffs $X = Y = 3.95$. See main text for more details.

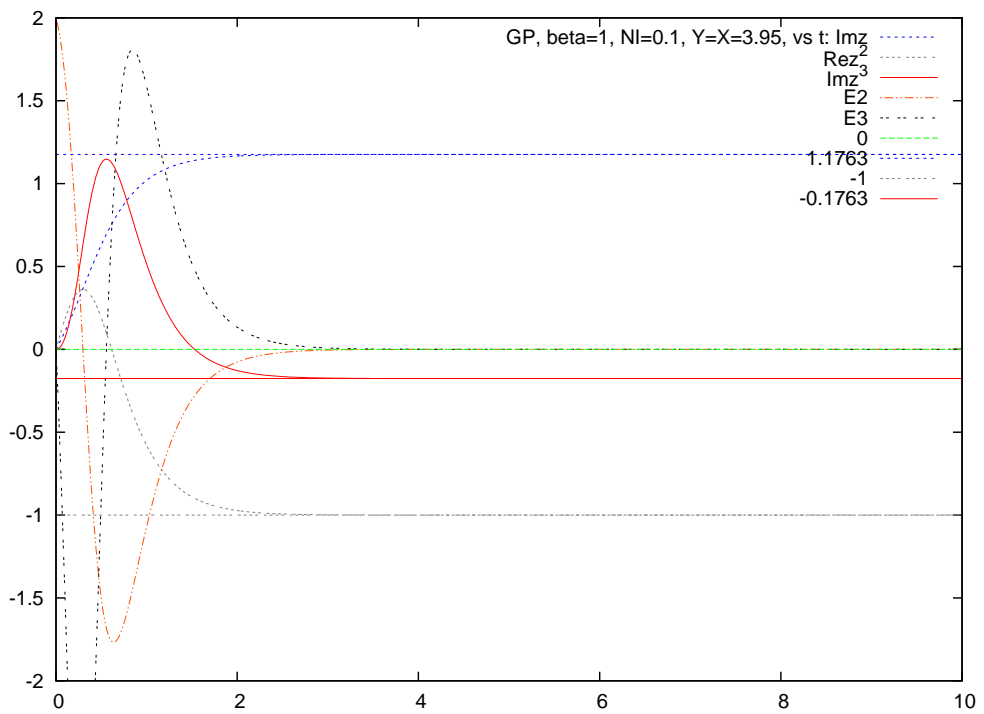


Figure 14: As in Fig. 13 for $N_I = 0.1$.

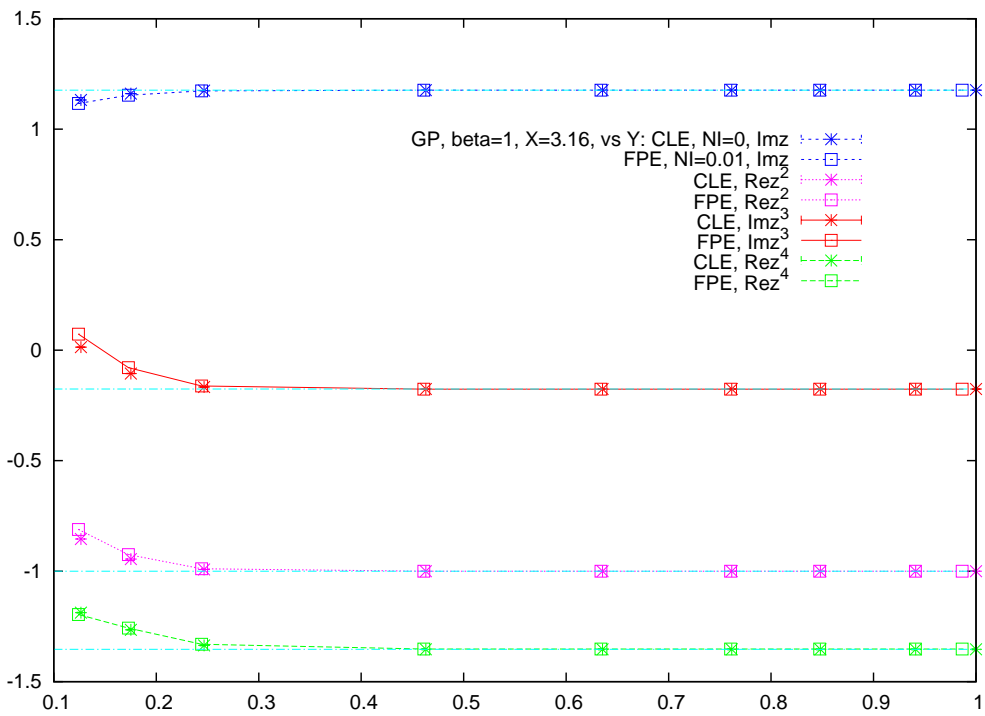


Figure 15: GP model: Cutoff (Y)dependence for $\beta = 1$ and $N_I = 0$ (CLE) and $N_I = 0.01$ (FPE)